How to cite: *Angew. Chem. Int. Ed.* **2023**, *62*, e202311639
doi.org/10.1002/anie.202311639

VIP **Foldamers** *Very Important Paper*

High-Affinity Hybridization of Complementary Aromatic Oligoamide Strands in Water

Victor Koehler, Gabrielle Bruschera, Eric Merlet, Pradeep K. Mandal, Estelle Morvan, Frédéric Rosu, Céline Douat, Lucile Fischer, Ivan Huc, and Yann Ferrand**

Abstract: We prepared a series of water-soluble aromatic oligoamide sequences all composed of a segment prone to form a single helix and a segment prone to dimerize into a double helix. These sequences exclusively assemble as antiparallel duplexes. The modification of the duplex inner rim by varying the nature of the substituents borne by the aromatic monomers allowed us to identify sequences that can hybridize by combining two chemically different strands, with high affinity and complete selectivity in water. X-ray crystallography confirmed the expected antiparallel configuration of the duplexes whereas NMR spectroscopy and mass spectrometry allowed us to assess precisely the extent of the hybridization. The hybridization kinetics of the aromatic strands was shown to depend on both the nature of the substituents responsible for strand complementarity and the length of the aromatic strand. These results highlight the great potential of aromatic hetero-duplex as a tool to construct non-symmetrical dynamic supramolecular assemblies.

Molecular self-sorting is a process through which molecules self-organize into distinct entities.[1] This molecular programming achieves high-fidelity recognition and potentially function within complex mixtures. Over the years, chemists have established molecular codes that allow synthetic molecules to preferentially engage in interactions with specific partners. In nature, self-sorting of oligomeric peptidic and nucleotidic strands into duplexes is both common and essential.[2] In particular, social self-sorting, that is, the selective recognition of different yet complementary entities is critical to information storage, replication and transfer in living systems. This has inspired chemists to design artificial oligomers that form sequence-selective duplexes mimicking their natural counterparts. For example, linear oligomers may assemble when they possess sequence-complementary arrangements of hydrogen bond donors and acceptors.[3] However, combining such sequence complementarity with shape control proved to be more challenging. Some self-assembled homomeric double helices have been reported eventually nucleated by anions or cations,[4] yet heteromeric double helices (i.e. folded duplexes composed of two different strands) are far less common and often not produced quantitatively.[5] In other words, establishing a reliable pairing mode between two different folded strands distinct from nucleotidic duplexes or peptidic assemblies has been a rarely met challenge, even more so in water. In this context, the hetero-duplexes based on aminidium–carboxylate[6] (or phosphate[7]) pairing in organic solvents developed by Yashima et al. constitute a unique and significant example. We describe herein the selective and quantitative hybridization of two chemically inequivalent artificial molecular strands in water to form hetero-duplexes. Our design is based on aromatic oligoamide double helices that rely on two sorts of intermolecular interactions, one perpendicular to the helix axis and dominated by steric effects, and the other parallel to the helix axis and associated with aromatic staking.

The association of aromatic helices into helical dimers in organic solvents is well documented.[5,8] We have also shown that water may enhance double helix formation.[9] This was assigned to the hydrophobic effect via a lesser exposure of the aromatic surfaces to water in the duplex than in two single helices. The present study focuses on oligoamide sequences combining 8-amino-2-quinolinecarboxylic acid (Q), which codes for a narrow helix diameter and 7-amino-2-quinolinecarboxylic acid bearing a substituent X in position 8 (Q^X), which codes for a wider helix diameter (Figure 1b–e). Q_n segments fold into single helices whereas $Q^X{}_m$ segments have a strong propensity to form helical dimers in which all X groups converge towards the helix cavity. $Q^X{}_mQ_n$ may thus self-associate as an anti-parallel double helix of two $Q^X{}_m$ segments with a Q_n single helix at each end (Figure 1a).[9] We devised that modifications of the double helix inner cavity, i.e. varying X on the edge of the aromatic core, may allow for the hybridization of two distinct strands

[*] Dr. V. Koehler, G. Bruschera, E. Merlet, Dr. L. Fischer, Dr. Y. Ferrand
CBMN (UMR 5248) Univ. Bordeaux, CNRS, Bordeaux Institut National Polytechnique
2 rue Escarpit 33600 Pessac (France)
E-mail: yann.ferrand@u-bordeaux.fr

Dr. P. K. Mandal, Dr. C. Douat, Prof. I. Huc
Department Pharmazie, Ludwig-Maximilians-Universität München
Butenandtstr. 5–13, 81377 München (Germany)
E-mail: ivan.huc@cup.lmu.de

E. Morvan, Dr. F. Rosu
IECB, UAR3033 Univ. Bordeaux, CNRS, INSERM
2 rue Robert Escarpit, 33600 Pessac (France)

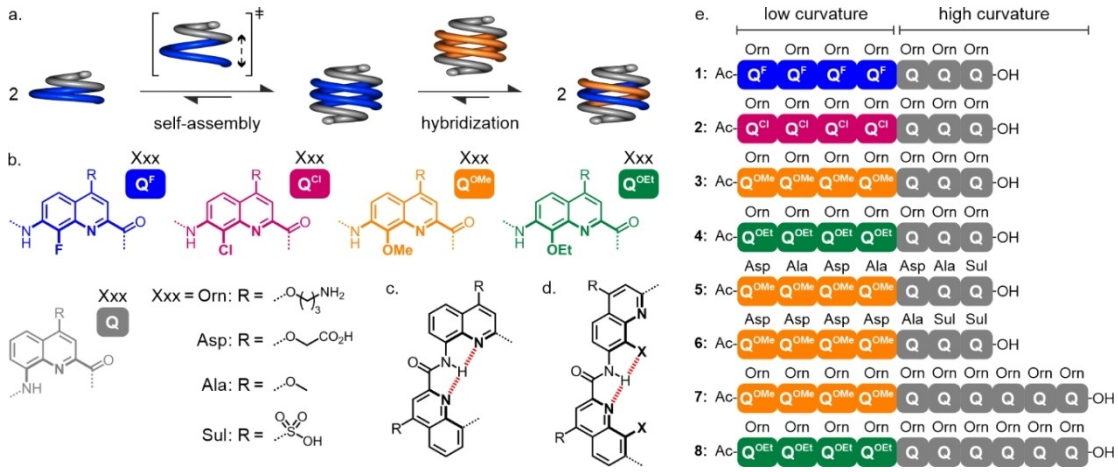

Figure 1. a) Schematic representation of: (left) the self-assembly of a single helix into an antiparallel homomeric double helix followed by (right) its hybridization with a chemically different strand forming a heteromeric double helix. b) Color coded formulae and associated abbreviations of aromatic amino acid monomers. Representation of the helical curvature of: c) a Q_2 dimer (2.5 units/turn); and d) a Q^X_2 dimer (X = F, Cl, OMe or OEt, 4 units/turn). e) Oligoamide sequences **1**–**8**.

with different X groups able to engage in attractive contacts or able to minimize repulsions.

Synthetic methods and protocols for new monomers and oligomers are described in detail in the Supporting Information. We first designed a series of $Q^X_4Q_3$ sequences equipped with cationic water-solubilizing side chains in position 4 of the monomers. Thus, **1**–**4** differ only by the nature of the X group of Q^X monomers. X can be more or less bulky (F < Cl < OMe < OEt) and can present an electron donating (OMe, OEt) or withdrawing (F, Cl) character. Typically, the sequences were synthesized either manually, or with an automated synthesizer, on low-loading ProTide® PEG-PS resin using conventional Fmoc-based chemistry under microwave irradiation or by controlled induction heating.[10] The acids were activated using either Ghosez reagent before the coupling or in situ using Appel coupling conditions. Fmoc deprotection with DBU was preferred over piperidine in DMF as some Q^X monomers were poorly reactive to the latter. All sequences were obtained as their respective trifluoroacetate ammonium salts with excellent purity and very good amounts (82–94 % with respect to theoretical loading, see Supporting Information) without HPLC purification.

The propensity of sequences **1**–**4** to form double helices was assessed by ^{1}H NMR. In DMSO-d_6, a solvent known to disfavor double helix formation, sequences **1**, **3**, and **4** revealed a unique set of resonances that were assigned to a single helix (Figures 2a, 2c, S1–S4). In contrast, still in DMSO-d_6, **2** weakly aggregates with a $K_{dim} = 1.6\times10^3$ L.mol^{-1}. Upon adding water to the DMSO-d_6 solutions of **1**–**4**, a new set of well-resolved high-field-shifted resonances, characteristic of double helix formation, emerged (Figures 2b, 2d, S1–S5). The number of resonances indicated that the double helices have two equivalent strands. At 1 mM, the amount of water required for the onset of aggregation varied with X, from 0 %, less than 15 %, less than 35 %, and less than 55 % for **2**, **1**, **3** and **4**,

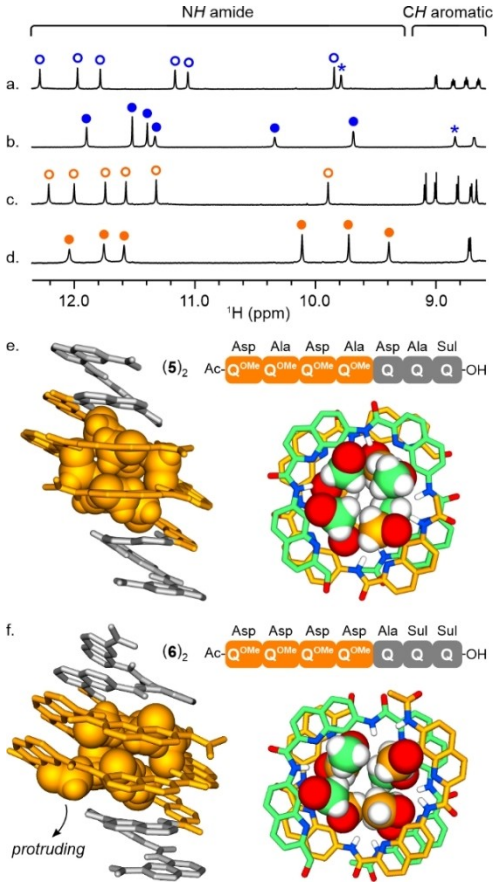

Figure 2. Excerpts of ^{1}H NMR spectra (700 MHz, 323 K) of a) **1** (1 mM, DMSO-d_6); b) (**1**)$_2$ (0.5 mM, H_2O/D_2O 95 : 5 vol/vol); c) **3** (1 mM, DMSO-d_6); d) (**3**)$_2$ (0.5 mM, H_2O/D_2O 95 : 5 vol/vol). X-ray structures of the antiparallel homomeric double helices: e) (**5**)$_2$ and f) (**6**)$_2$. Methoxy groups are shown in space filling representation. In the side views, Q and Q^{OMe} are colored in grey and orange, respectively. In the top view (slice), each strand is shown with a distinct color for clarity (green, orange). Side chains and included solvent molecules have been removed for clarity.

respectively, indicating different duplex stabilities. However, in pure water, the duplex was the only detectable species for all compounds. Upon diluting solutions of $(\mathbf{1})_2$ or $(\mathbf{3})_2$ in water down to 20 μM, no monomer could be observed providing a minimal estimate of $K_{dim} > 10^8$ L.mol^{-1} (Figures S6–S9). This behavior was unchanged in the presence of a 50 mM ammonium acetate buffer. Native electrospray mass spectrometry (ESI-MS) using soft instrumental conditions confirmed the formation of $(\mathbf{1})_2$ and $(\mathbf{3})_2$ albeit mixed with monomers **1** and **3**. We inferred that some duplex dissociation occurred during ionization. Additionally, ion mobility MS analysis confirmed collision cross-section profiles that matched well with the double and single helices (Figures S10–S11).

Structural information at the atomic scale on the homomeric double helix was obtained from the solid state structures[11] of sequences **5** and **6**, two analogues of **3** bearing short neutral and anionic side chains more prone to crystallization than the flexible ornithine-like side chains of **3** (Figure 1e). The structures confirmed the anticipated antiparallel arrangement of the strands as well as the single helical and double helical nature of the Q_3 and $Q^{OMe}{}_4$ segments, respectively (Figure 2e, 2f). In both structures, the helix cavity is filled with a crowded arrangement of eight methoxy groups, which pack more tightly in $(\mathbf{5})_2$ than in $(\mathbf{6})_2$ (Figure S12).

Next, we assessed the propensity of homodimers **1**–**4** to form heteromeric double helices. Hybridization was followed using ^{1}H NMR and also ^{19}F NMR for **1**. Upon incubating $(\mathbf{1})_2$ with $(\mathbf{2})_2$ in water (H_2O/D_2O−95:5 vol/vol) for 12 hours at 298 K no change could be observed (Figure S13). Heating to 323 K led to the appearance of a new set of sharp signals with twice the number of resonances (12 amide NHs) as $(\mathbf{1})_2$ or $(\mathbf{2})_2$ (6 amide NHs each) suggesting the formation of heteroduplex **1·2** (Figures S13d, S14b). Thermodynamic equilibrium was reached after 12 hours and revealed that the proportion of **1·2** reached 78 %. Similarly, mixing $(\mathbf{2})_2$ with $(\mathbf{3})_2$ yielded **2·3** up to a proportion of 87 % (Figure S15). In both cases, the proportion of heteroduplex exceeded that of a statistical distribution (50 %), hinting at a better steric or electronic complementarity than in homomeric double helices. Remarkably, upon mixing $(\mathbf{1})_2$ with $(\mathbf{3})_2$, the ^{1}H and ^{19}F resonances of the homomeric double helices completely vanished within 5 minutes at 323 K, and were fully replaced by a unique set of signals corresponding to **1·3** (Figures 3a, b, d and S16, S17). Consistent with the high stability of $(\mathbf{1})_2$ and $(\mathbf{3})_2$, no dissociation of **1·3** was detected upon dilution down to 20 μM in water or buffered water (Figures S18, S19). The quantitative formation of **1·3** indicates that the equilibrium constant K' between $(\mathbf{1})_2 + (\mathbf{3})_2$ and $2\times\mathbf{1\cdot3}$ is larger than 2500 (see the Supporting Information). Accordingly, a minimum estimate for the stabilization of the heteroduplex **1·3** was determined as $\Delta G < -19.4$ kJ/mol. Finally the self-sorting ability of the aromatic sequences bearing fluorine, methoxy or chlorine substituents was evaluated by ^{1}H NMR. Mixing $(\mathbf{1})_2$, $(\mathbf{2})_2$ and $(\mathbf{3})_2$ in a 1:1:1 ratio in $CDCl_3$ showed the progressive disappearance of $(\mathbf{1})_2$ and $(\mathbf{3})_2$—the concentration of $(\mathbf{2})_2$ remained unchanged—together with the quantitative formation of the heteroduplex **1·3**, without detection of **1·2** or **2·3** (Figure S31).

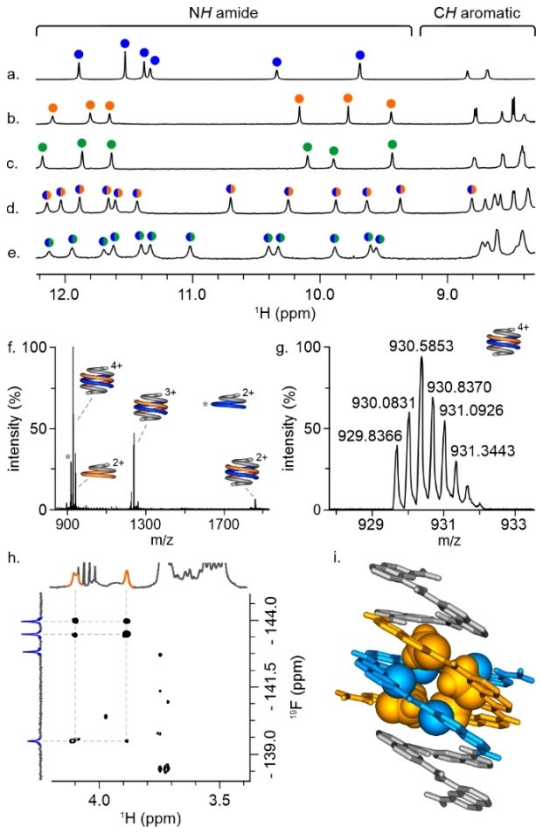

Figure 3. Excerpts of ^{1}H NMR spectra (H_2O/D_2O−95:5 vol/vol, 700 MHz, 323 K) of: a) $(\mathbf{1})_2$ (0.5 mM); b) $(\mathbf{3})_2$ (0.5 mM); c) $(\mathbf{4})_2$ (0.5 mM); d) **1·3** (1 mM); e) **1·4** (1 mM). Amide resonances of $(\mathbf{1})_2$, $(\mathbf{3})_2$, $(\mathbf{4})_2$, **1·3** and **1·4** are marked with blue, orange, green, blue/orange and blue/green circles, respectively. f), g) High resolution ElectroSpray Ionization Mass Spectrum (ESI-MS) of **1·3**. h) Zoom of ^{1}H-^{19}F HOESY NMR spectra (H_2O/D_2O−95:5 vol/vol, 400 MHz, 323 K) of **1·7**. Resonances corresponding to fluorine atoms are denoted in blue whereas those of methoxy groups ($OC\underline{H}_3$) are shown in orange, respectively. i) Energy minimized molecular models (MMFFs) of **1·3**. Fluorine atoms and methoxy groups are shown in space-filling representation. Q, Q^F and Q^{OMe} are colored in grey, blue, and orange, respectively. Side chains have been removed for clarity.

The hybridization of **1·3** was also confirmed by native electrospray mass spectrometry. The heteromeric double helix was unambiguously detected at $m/z = 1858.6$, 1239.4, 929.8 (2+, 3+ and 4+ species) (Figures 3f, 3g and S22). Single helices **1** and **3** were also detected as a consequence of dissociation during ionization and despite the smooth conditions.

Detailed structural information could not be gathered using crystallography. Nevertheless, hybridization was confirmed using ^{1}H-^{19}F Heteronuclear Overhauser Effect SpectroscopY (HOESY) which can assess the spatial proximity between ^{1}H and ^{19}F nuclei. For these experiments, we used dimer **1·7**, an analogue of **1·3** bearing seventeen hydrosolubilizing ammonium side chains vs fourteen for **1·3**. The better solubility of **1·7** allowed for a higher concentration in water and increase of signal-to-noise ratio for HOESY

experiments. The ^{1}H-^{19}F HOESY spectrum demonstrated dipolar couplings between fluorine atoms of the Q^{F} units and the methyl groups of the Q^{OMe} units, thus confirming the proximity of these functional groups in the cavity of the heteromeric double helix (Figures 3h, S20). A molecular model of **1·3** was built, revealing shape complementarity between the small fluorine atoms and the methoxy groups whose position may vary through rotation about C_{ar}–O bonds (Figure 3i). The crowding of methoxy groups in $(\mathbf{3})_2$, $(\mathbf{5})_2$, and $(\mathbf{6})_2$ (Figures 2, S21, S30 and S43) is released in **1·3**, suggesting that sterics contribute to hybridization (Figure S12). The absence of steric bulk within $(\mathbf{2})_2$ would explain why it hybridizes less efficiently with $(\mathbf{1})_2$. The weak hybridization between $(\mathbf{2})_2$ and $(\mathbf{3})_2$ could also reflect a weaker steric drive (crowding within $(\mathbf{3})_2$ is less efficiently released with chlorine than fluorine), or that other effects than sterics favor for the formation of **1·3**, for example electronic effects specific to fluorine.

The hybridization kinetics were examined further by increasing the length of the *C*-terminal single helical Q_n segments, or by increasing the substituent size in position 8 of the Q^{X} units. Sequences **4**, **7**, and **8** served that purpose (Figure 1e). Upon mixing $(\mathbf{1})_2$ and $(\mathbf{7})_2$, the elongated version of $(\mathbf{3})_2$, the formation of **1·7** was followed by ^{1}H and ^{19}F NMR (Figures 4b, c, f and S23–25). We found that the heteroduplex formed quantitatively over 90 minutes at 323 K in H_2O/D_2O (95:5 vol/vol). By comparison, the formation of **1·3** took less than five minutes (Table S1). The slower kinetics with **7** suggest a remote effect of the single helical segments which may stabilize the central duplex. Such remote effects have been observed before.[12]

Effects were also strong with Q^{OEt}-containing sequences **4** and **8**. Mixing $(\mathbf{1})_2$ with $(\mathbf{4})_2$ produced **1·4** at a rate too fast to be monitored, as observed with **1·3**. When using longer oligomer $(\mathbf{8})_2$, the formation of **1·8** was slower, yet it was complete after only 15 minutes, that is, six times quicker than for **1·7** (Figures 4, S26–S29). Molecular models of heteromeric **1·7** and **1·8** (Figure S30) showed a good shape-complementarity, and compact well-folded helices for both hetroduplexes. In contrast, steric crowding of the ethoxy groups within $(\mathbf{8})_2$ was considerable, leading to distortions of the double helix and ethoxy groups protruding from the cavity (Figure S30). The faster kinetics with $(\mathbf{8})_2$ may thus result from its lower stability with respect to $(\mathbf{7})_2$, facilitating the exchange with complementary strands. Nevertheless, the prevalent exchange mechanism is yet to be established, namely, completely dissociative (between two single helices), through direct exchange (between two double helices), or hybrid (either between two double helices or between a dissociated single and a double helix). Double helix formation is presumed to proceed with limited perturbation of the helical structure via the slipping of the two single helices into one another in an eddy-like process.[13] Whether this allows for a direct exchange of strands, as seen in other systems,[6c] is not known. In any case, helix length and the bulk in the cavity emerge as convenient parameters to fine-tune the kinetics of exchange.

In summary, we established quantitative hybridization of aromatic helices in water using interacting groups within the duplex cavity. The heterodimers show high stability even for the short sequences studied and their kinetics of formation may be adjusted. We believe that this high level of self-sorting in water will be useful when combined with biomolecules for biomaterial engineering. The hybridization may give access to advanced biomaterials with low symmetry.

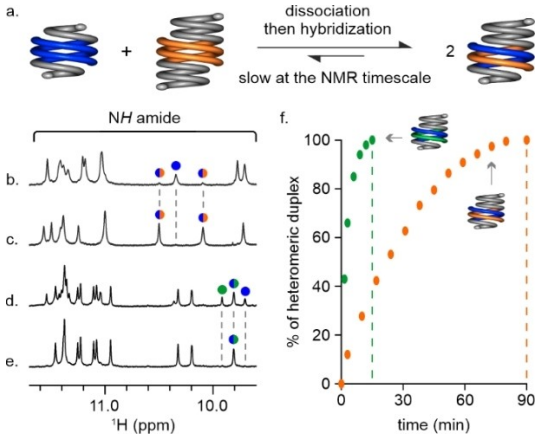

Figure 4. a) Schematic representation of the hybridization between two strands of different lengths. Excerpts of ^{1}H NMR spectra (H_2O/D_2O–95:5 vol/vol, 700 MHz, 323 K) of an equimolar mixture of $(\mathbf{1})_2$ (0.5 mM) and $(\mathbf{7})_2$ (0.5 mM) after: b) 3 min; c) 90 min (thermodynamic equilibrium). Same experiment with $(\mathbf{1})_2$ (0.5 mM) and $(\mathbf{8})_2$ (0.5 mM) after: d) 3 min; e) 15 min (thermodynamic equilibrium). Amide signals of $(\mathbf{1})_2$, $(\mathbf{8})_2$, **1·7** and **1·8** are marked with blue, green, blue/orange and blue/green circles, respectively. f) Time traces of the hybridization process in water of **1·7** (orange circles) and **1·8** (green circles).

Acknowledgements

We thank the "Agence Nationale de la Recherche" for funding the project ANR-19-CE07-0034 and the France-Germany International Research Project "Foldamers Structures and Functions" (IRP FoldSFun). This work benefited from the facilities of the Biophysical and Structural Chemistry platform at IECB, CNRS UAR3033, and Bordeaux University, France. We thank G. Leonard (ID30b, ESRF, Grenoble) and S. Panneerselvam (P14 operated by EMBL at PETRA III, DESY, Hamburg) for assistance during data collection at synchrotron beamlines.

Conflict of Interest

The authors declare no conflict of interest.

Data Availability Statement

The data that support the findings of this study are available in the supplementary material of this article.

Keywords: Aromatic Oligoamide · Artificial Hybridization · Double Helix · Foldamer · Self-Assembly

[1] a) J.-M. Lehn, *Science* **2002**, *295*, 2400; b) M. M. Safont-Sempere, G. Fernández, F. Würthner, *Chem. Rev.* **2011**, *111*, 5784.

[2] a) J. D. Watson, F. H. Crick, *Nature* **1953**, *171*, 737; b) B. A. Wallace, K. Ravikumar, *Science* **1988**, *241*, 182; c) D. N. Woolfson, *Adv. Protein Chem.* **2005**, *70*, 79.

[3] a) B. Gong, *Acc. Chem. Res.* **2012**, *45*, 2077; b) A. E. Stross, G. Iadevaia, C. A. Hunter, *Chem. Sci.* **2016**, *7*, 94; c) D. Núñez-Villanueva, C. A. Hunter, *Chem. Sci.* **2017**, *8*, 206; d) A. E. Stross, G. Iadevaia, G. D. Núñez-Villanueva, C. A. Hunter, *J. Am. Chem. Soc.* **2017**, *139*, 12655; e) P. Troselj, P. Bolgar, P. Ballester, C. A. Hunter, *J. Am. Chem. Soc.* **2021**, *143*, 8669; f) E. A. Archer, M. J. Krische, *J. Am. Chem. Soc.* **2002**, *124*, 5074; g) E. A. Archer, N. T. Goldberg, V. Lynch, M. J. Krische, *J. Am. Chem. Soc.* **2000**, *122*, 5006.

[4] a) E. Yashima, N. Ousaka, D. Taura, K. Shimomura, T. Ikai, K. Maeda, *Chem. Rev.* **2016**, *116*, 13752; b) D. Haldar, C. Schmuck, *Chem. Soc. Rev.* **2009**, *38*, 363; c) J. Li, J. A. Wisner, M. C. Jennings, *Org. Lett.* **2007**, *9*, 3267; d) H. Goto, H. Katagiri, Y. Furusho, E. Yashima, *J. Am. Chem. Soc.* **2006**, *128*, 7176; e) H. Sugiura, R. Amemiya, M. Yamaguchi, *Chem. Asian J.* **2008**, *3*, 244; f) C. J. Massena, D. A. Decato, O. B. Berryman, *Angew. Chem. Int. Ed.* **2018**, *57*, 16109; g) Y. Liu, F. C. Parks, W. Zhao, A. H. Flood, *J. Am. Chem. Soc.* **2018**, *140*, 15477; h) F. C. Parks, Y. Liu, S. Debnath, S. R. Stutsman, K. Raghavachari, A. H. Flood, *J. Am. Chem. Soc.* **2018**, *140*, 17711; i) R. Kramer, J.-M. Lehn, A. Marquis-Rigault, *Proc. Natl. Acad. Sci. USA* **1993**, *90*, 5394.

[5] a) C. Zhan, J.-M. Léger, I. Huc, *Angew. Chem. Int. Ed.* **2006**, *45*, 4625; b) Q. Gan, F. Li, G. Li, B. Kauffmann, J. Xiang, I. Huc, H. Jiang *Chem. Commun.* **2010**, *46*, 297; c) M. L. Singleton, G. Pirotte, B. Kauffmann, Y. Ferrand, I. Huc, *Angew. Chem. Int. Ed.* **2014**, *53*, 13140; d) V. C. M. Smith, J.-M. Lehn, *Chem. Commun.* **1996**, 2733.

[6] a) Y. Tanaka, H. Hatagiri, Y. Furusho, E. Yashima, *Angew. Chem. Int. Ed.* **2005**, *44*, 3867; b) H. Ito, Y. Furusho, E. Yashima, *J. Am. Chem. Soc.* **2008**, *130*, 14008; c) H. Yamada, Z. Q. Wu, Y. Furusho, E. Yashima, *J. Am. Chem. Soc.* **2012**, *134*, 9506.

[7] M. Thiele, F. Octa-Smolin, S. Thölke, C. Wölper, J. Linders, C. Mayer, G. Haberhauer, J. Niemeyer, *Chem. Commun.* **2021**, *57*, 9842.

[8] a) V. Berl, I. Huc, R. G. Khoury, M. J. Krische, J. M. Lehn, *Nature* **2000**, *407*, 720; b) Q. Gan, C. Bao, B. Kauffmann, A. Grélard, J. Xiang, S. Liu, I. Huc, H. Jiang, *Angew. Chem. Int. Ed.* **2008**, *47*, 1715; c) Q. Gan, X. Wang, B. Kauffmann, F. Rosu, Y. Ferrand, I. Huc, *Nat. Nanotechnol.* **2017**, *12*, 447.

[9] J. Shang, Q. Gan, S. J. Dawson, F. Rosu, H. Jiang, Y. Ferrand, I. Huc, *Org. Lett.* **2014**, *16*, 4992.

[10] V. Corvaglia, F. Sanchez, F. S. Menke, C. Douat, I. Huc, *Chem. Eur. J.* **2023**, *29*, 202300898.

[11] Deposition numbers 2216832 (**(5)$_2$**) and 2232111 (**(6)$_2$**) contain the supplementary crystallographic data for this paper. These data are provided free of charge by the joint Cambridge Crystallographic Data Centre and Fachinformationszentrum Karlsruhe Access Structures service.

[12] Y. Ferrand, N. Chandramouli, A. M. Kendhale, C. Aube, B. Kauffmann, A. Grélard, M. Laguerre, D. Dubreuil, I. Huc, *J. Am. Chem. Soc.* **2012**, *134*, 11282.

[13] a) Zerbetto, Venturini, *J. Am. Chem. Soc.* **2004**, *126*, 2362; b) *J. Phys. Chem. B* **2017**, *121*, 10064.

Manuscript received: August 10, 2023
Accepted manuscript online: October 7, 2023
Version of record online: October 23, 2023